

Review

The process of folding proteins into membranes: Challenges and progress

Ann Marie Stanley, Karen G. Fleming *

T. C. Jenkins Department of Biophysics, Johns Hopkins University, 3400 North Charles Street, Baltimore, MD 21218, USA

Received 27 June 2007, and in revised form 17 September 2007

Available online 22 October 2007

Abstract

Just 25 years ago the Anfinsen thermodynamic hypothesis was shown to be valid for membrane proteins. Despite the complex biological machinery required for their *in vivo* assembly and in face of the chemically heterogeneous, anisotropic nature of their biological lipid bilayer “solvent”, the evidence continues to suggest that membrane proteins are equilibrium structures. The progress in finding conditions *in vitro* to investigate the physical origins of their stabilities is the focus of this article. We catalogue *in vitro* folding studies in detergent micelles and in lipid bilayers. We consider the unique technical obstacles to folding studies of membrane proteins, and we highlight the progress that has been made in quantitative descriptions of membrane protein stability.

© 2007 Elsevier Inc. All rights reserved.

Keywords: Membrane protein; Thermodynamics; Protein folding

A pressing challenge in modern biology is to understand how protein sequences encode biological activity. Since the first and fundamental task common to every protein sequence is to fold into its functional state, the prediction of a protein’s native conformation from its amino acid sequence is an important hurdle to be overcome. Solving this so-called protein-folding problem will provide researchers with the expertise to predict structures from sequence, to predict structural changes in response to genetic mutations, to design novel protein folds and functions, and to rationally engineer safe and effective pharmaceutical agents. These skills will be powerful tools in the fields of medicine, structural biology, biotechnology, bio-engineering, and protein design.

Progress in understanding the folding of membrane proteins has lagged far behind that of soluble proteins, whose folding stabilities and kinetics have been studied for decades. Early in the history of the soluble protein-folding field, it was recognized that the native conformation of a protein resides in a Gibbs free energy minimum. Elegant

experiments pioneered by Anfinsen almost a half century ago demonstrated that a denatured protein could be refolded *in vitro* to its native conformation in the absence of any energy input [1]. Consequently, not only must the native structure be at a free energy minimum, the unique three-dimensional conformation of a protein must also somehow be encoded by its linear amino acid sequence. This postulate, referred to as the thermodynamic hypothesis of folding, describes the folding of numerous soluble proteins with few exceptions (i.e., kinetically trapped proteins like α -lytic protease [2]).

Despite their importance and abundance, the molecular assembly process for membrane proteins is still a largely unexplored field: there are fewer than 100 publications indexed by Pubmed that contain the phrase “membrane protein folding” in the abstract or title whereas there are >24,000 occurrences of the phrase “protein folding”, presumably dominated by soluble proteins (Fig. 1). Initially, it was unclear whether the thermodynamic hypothesis would extend to the folding of membrane proteins. The biological lipid bilayer in which membrane proteins reside is an unusual and anisotropic macromolecular solvent. The chemical composition of the membrane varies greatly

* Corresponding author. Fax: +1 410 516 4118.

E-mail address: Karen.Fleming@jhu.edu (K.G. Fleming).

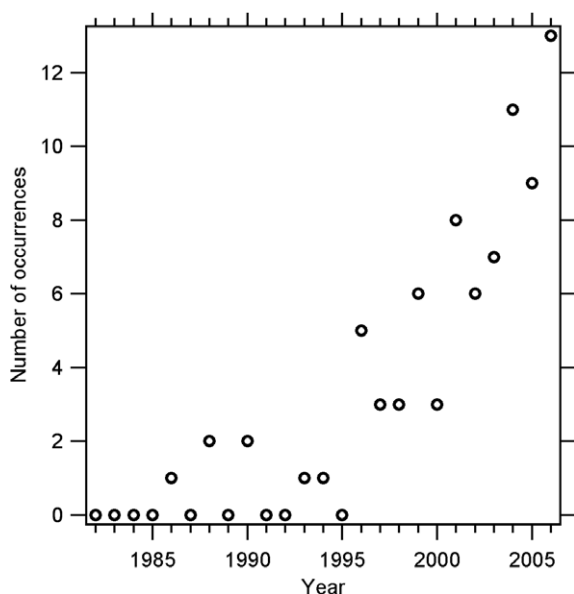


Fig. 1. Occurrences of the phrase “membrane protein folding” in publications indexed by Pubmed. The number of papers using the phrase “membrane protein folding” in either the title or the abstract are plotted as a function of publication year. The total number through 2006, the latest full year for which data were available, equals 86.

along the normal, but by virtue of the bilayer structure it also contains an approximate twofold symmetry along this axis [3,4]; even so, membrane proteins are not randomly inserted into membranes but are found *in vivo* with a defined transbilayer topology [5–8]. Helical membrane proteins are found in most eukaryotic membranes and in the inner membranes of bacteria; their *in vivo* assembly into membranes requires the assistance of a special cellular machine known as the translocon, and the process is associated with mechanical work, either from the translocation of the ribosome or from ATP¹ hydrolysis [9]. In contrast, transmembrane β -barrel membrane proteins found in bacterial outer membranes must traverse through the translocon in the inner bacterial membrane and subsequently

¹ Abbreviations used: ATP, adenosine 5'-triphosphate; β OG, octyl β -D-glucopyranoside; β ME, β -mercaptoethanol; BB, β -barrel; BR, bacteriorhodopsin; C8-POE, octyl polyoxyethylene monoether; C14SB, *n*-tetradecyl-*N,N*-dimethyl-3-ammonio-1-propanesulfonate; CD, circular dichroism; CL, cardiolipin; DAGK, diacylglycerol kinase; DBG, dibutylglycerol; DM, *n*-decyl β -D-maltoside; D-states, denatured state ensemble; DTT, dithiothreitol; EDTA, ethylenediaminetetraacetic acid; EGTA, ethylenedis(oxyethylenenitrilo)tetraacetic acid; GdnHCl, guanidine hydrochloride; IB, inclusion body; KCl, potassium chloride; KPi, potassium phosphate; LiCl, lithium chloride; LHCIIb, light harvesting complex subunit IIb; MOPS, 3-(*N*-Morpholino)-propanesulfonic acid; NaB, sodium borate; NaCl, sodium chloride; NADH, nicotinamide adenine dinucleotide, reduced form; NaPi, sodium phosphate; oPOE, same as C8-POE; OMPA, outer membrane phospholipase A; OmpA, outer membrane protein A; OmpF, outer membrane porin F; OmpX, outer membrane protein X; PEP, phosphoenolpyruvate; PIPES, piperazine-*N,N'*-bis(2-ethanesulfonic acid); POPC, palmitoyl-oleoyl-phosphatidylcholine; POPG, palmitoyl-oleoyl-phosphatidylglycerol; SDS, sodium dodecylsulfate; SDS-PAGE, sodium dodecyl sulfate-polyacrylamide gel electrophoresis.

cross the periplasm to reach their final destination of folding and assembly. Notably, the periplasm is exposed to both the inner and outer membranes; nevertheless, transmembrane β -barrels are selectively incorporated only into the outer membrane *in vivo* by a process that is poorly understood [10] but that is likely to involve an evolutionarily conserved proteinaceous outer membrane folding apparatus [11–13]. Because of the asymmetric and intricate biosynthetic assembly and insertion of these molecules, it may not have been surprising if membrane proteins were “kinetically” trapped *in vivo* by the assembly process and if the Anfinsen hypothesis failed to hold for them [14].

However, as early as 1981 evidence emerged to support the hypothesis that membrane proteins are equilibrium structures. Work from the Khorana group showed that bacteriorhodopsin (BR) could be renatured from a fully-denatured, acid-unfolded state; the refolded protein could bind its retinal chromophore; and full activity could be recovered [15]. The same study also demonstrated that proteolytic fragments of bacteriorhodopsin could assemble into a functional molecule [15]. Subsequent crystallographic work unequivocally confirmed that the reassembled BR adopted a native conformation [16]. Furthermore, the complementation experiments suggested that the water-exposed loops interconnecting transmembrane helices were not essential for specifying the tertiary fold of membrane proteins; rather, these experiments suggested that interactions within the membrane-embedded domain were key for folding specificity [15]. The renaturation of bacteriorhodopsin was the first evidence that—as is the case for soluble proteins—membrane proteins exist at a free energy minimum.

Subsequently, it has been shown that numerous helical membrane proteins can be functionally complemented by polypeptide fragments and that the results can be extended to transmembrane β -barrels (reviewed in [17]). The thermodynamic hypothesis also appears to hold true for membrane β -barrels: OmpA, an archetypal transmembrane β -barrel, can be assembled from polypeptide fragments [18] or efficiently synthesized *in vivo* when the order of its strands is circularly permuted [19]. Moreover, it has been demonstrated that many outer membrane proteins can be renatured from a urea-unfolded state [20]. This ability of membrane proteins to achieve a native conformation by various folding pathways provides strong support that Anfinsen's thermodynamic hypothesis extends to membrane proteins. Thus, despite the complexities of their *in vivo* folding pathways, the observation that membrane proteins are equilibrium structures means that thermodynamic folding studies *in vitro* can be used to investigate their stabilities and to query how sequence changes influence their folds and energetics.

The requirements, challenges, and progress of *in vitro* investigations aimed at deciphering the physical origins of membrane protein stability are the focuses of this review article. As a starting point for these studies, it is useful to know the conditions that have been successful in folding

membrane proteins in the laboratory. Detergent micelles continue to be extremely useful tools for both structural and thermodynamic studies of membrane proteins, and Table 1 shows a compilation of the micelle conditions found to produce folded membrane proteins. More recently there is an increase in querying the ability of synthetic lipid bilayers to support membrane protein folding *in vitro*, and Table 2 shows successful lipid bilayer conditions. We will use the information in both Tables 1 and 2 as we consider the progress and prospects of taking membrane protein folding studies to the next level to obtain their free energies of folding. Two principal factors are required: (1) simultaneous population of the folded and unfolded states under conditions that can somehow be related to the folding conditions where the free energy quantity is desired; and (2) solution conditions wherein the reaction is fast enough to reach equilibrium.

Requirements for stability studies *in vitro*

Population of the unfolded state

The Gibbs free energy of folding for a membrane protein can be determined when the concentrations of the native and unfolded states of a protein population are simultaneously known and are reversibly interchanging within the experimental timescale. Fig. 2 shows a cartoon of the most extensively studied *in vitro* folding reactions for transmembrane β -barrel and α -helical proteins. Following the convention of the soluble protein field, the free energy change will be written as a free energy of unfolding, ΔG_U , which will have positive values for stable native folds:

$$\Delta G_U = -RT \ln K_U = -RT \ln \frac{[U]}{[N]}$$

where R equals the gas constant, T equals the temperature in K, and K_U is the equilibrium constant for unfolding that equals the ratio of the concentrations of the unfolded, $[U]$; and folded, $[N]$, membrane protein conformations. As is true for soluble proteins, under folding conditions the equilibrium between the native and unfolded states of a membrane protein lies far in favor of the folded state, $[N] \gg [U]$; the unfolded population is present in such a minute fraction that it cannot usually be experimentally observed. To measure the free energy change for the folding reaction, the solution conditions must be adjusted to promote population of the unfolded state while maintaining a measurable population of the folded state. Herein lies the first challenge. The ideal denaturing agent would allow the investigator to easily move back and forth on the denaturation curve in a systematic way so that the free energy of change for unfolding could be experimentally determined under various conditions and be inferred by extrapolation of the equilibrium constant to the value in the absence of denaturant. In soluble protein studies, protein stability has been shown to depend linearly on the concentration of denaturant [21–23], and key membrane protein stability

studies suggest that the denaturant dependence of membrane proteins can also be a linear function of denaturant [24,25], although there is no solid theoretical understanding of why this should be the case. Nevertheless, one of the first hurdles to be overcome in studies of any particular membrane protein *in vitro* is to find favorable denaturation conditions that will facilitate this type of analysis.

Denaturation by pH and temperature

Taking cues from the soluble protein-folding field, chemical denaturants, pH, and temperature have all been used as denaturants in stability studies of membrane proteins. As mentioned previously, the use of acid to promote the unfolded state of bacteriorhodopsin was key in proving the Anfinsen hypothesis for membrane proteins [15], however, the free energy change for BR folding could not be determined in those experiments because its renaturation required passage through an SDS-denatured form to reach the native state in bilayers. Further, there are no reports of equilibrium folding experiments using either acid or base in an incremental fashion to systematically and reversibly modify the equilibrium constant for folding of any membrane protein.

Similarly, elevated temperature also appears incapable of reversibly denaturing several archetypal membrane proteins, including the α -helical proteins bacteriorhodopsin [26–29], cytochrome *c* oxidase [30,31], band 3 protein [32,33], photosystem II [34], and the transmembrane β -barrel porin proteins [35]. The thermal denaturation profiles observed by differential scanning calorimetry were irreversible; some showed scanning rate dependencies; and collectively they revealed enthalpy and heat capacity changes much lower in magnitude than those expected for proteins of similar molecular weight [36]. Together these observations suggest that elevated temperature incompletely unfolds membrane proteins; this conclusion is corroborated by independent experiments demonstrating significant fractions of secondary structure that persisted in the “temperature-denatured” states of these membrane proteins [30,31,33,35]. Overall, the thermal denaturation profiles were most consistent with the aqueous loops of these membrane proteins unfolding while the membrane-embedded regions retained many of the native structural features. While these studies did establish the remarkable thermal stability possessed by many membrane proteins, they also suggested there was a limited utility to temperature as a denaturant to be applied systematically for reversible thermodynamic studies.

This conclusion might deserve reconsideration in light of a recently identified outlier from this consensus behavior, the monomeric porin OmpG. The thermal denaturation profile of OmpG reconstituted in β -octylglucoside micelles was measured using circular dichroism (CD) in which a single sharp loss of CD signal was obtained with increasing temperature [37]. The original CD signal was recovered when the temperature was lowered, showing that the folded

Table 1
Membrane protein folding conditions observed using detergent micelles

Protein	MW (kDa); Topology; Oligomeric state	Denaturant	Other components of unfolding buffer	Method of refolding	Optimal refolding buffer	Refolding detergent	Folding efficiency	Conformation of D-states in denaturant ^a	Aggregation state of D-states ^a	Source	Year published, Reference
OmpF	37; 16 BB; Trimer	2% SDS	None	6× dilution	150 mM KCl	Soybean lecithin/ 2% octyl-POE	20–80%	Helical in SDS (CD)	ND	<i>E. coli</i>	1990, [35]
OmpF	37; 16 stranded BB; Trimer	8 M urea	20 mM KPi, pH 7.3	Dilution	20 mM NaPi, pH 6.5	DMPC/CM mixed micelles	73% trimer	No regular structure (CD)	ND	<i>E. coli</i>	1996, [109]
OmpA	35; 8 stranded BB; Monomer	0.05% SDS, 100 °C 10 min	75 mM Tris–HCl, pH 7.5	Addition of solid βOG	75 mM Tris–HCl, pH 7.5	βOG	>90%	40% α-helix (Raman spectroscopy)	Monomer	<i>E. coli</i>	1990, [110]
OmpA	35; 8 stranded BB; Monomer	8 M urea	20 mM KPi, pH 7.3	Dilution	10 mM KPi, pH 7.3	βOG	80%	No regular structure (CD)	ND	<i>E. coli</i>	1992, [94]
OmpA171 (just the TM barrel region)	24; 8 stranded BB; Monomer	6 N GdnHCl	None	Dilution	0.6 M Arginine	Dilution into 5% C8-POE, 0.6 M arginine	ND	ND	ND	<i>E. coli</i>	1999, [111]
PhoE	37; 16 stranded BB; Trimer	None	<i>In vitro</i> translation mixture	Addition of detergent	ND	Triton X-100 or Nonidet P-40 or Triton N-101 or Triton X-114 all supported folding (Lubrol-WX, octylglucoside, Tween20, sodium deoxycholate did not work)	10–15% of protein folded	ND	ND	<i>In vitro</i> transcription of mature protein without signal sequence	1994, [112]
PorB class 3 protein	Not stated; predicted BB; predicted Trimer	8 M urea	50 mM Tris–HCl, pH 8.0, 1 mM EDTA, 100 mM NaCl	Dilution	50 mM Tris–HCl, pH 8.0, 1 mM EDTA, 100 mM NaCl	C14SB	ND	ND	ND, although final folding efficiency was higher if the concentration was 10 mg ml ⁻¹ or less	<i>Neisserial</i> open reading frames expressed in <i>E. coli</i>	1994, [113]
Neisserial porins	Not stated; predicted 16 stranded BB; predicted Trimer	8 M urea	50 mM Tris–HCl, 1 mM EDTA, 100 mM NaCl, pH 8.0	Dilution	5% SB3-14, 4 M urea	C14SB	ND	ND	Aggregation only when concentration exceeded 10 mg ml ⁻¹	<i>Neisserial</i> open reading frames expressed in <i>E. coli</i>	1994, [113]
OMPLA	31; 12 stranded BB; Monomer–Dimer	8 M urea	100 mM glycine, 20 mM Tris, pH 8.3, 2 mM EDTA	Rapid dilution	20 mM Tris, pH 8.3, 2 mM EDTA, 1.4 M Urea	10 mM Triton X-100	35–60%	No regular structure (CD)	ND	<i>E. coli</i>	1995, [99]
<i>H. influenzae</i> type b porin	38; predicted BB; predicted Trimer	Purified porin in 6 M urea was precipitated by dialysis against water, suspended in 1% SDS, boiled and cooled	50 mM Tris–HCl, pH 8.0	Fivefold dilution of protein with 0.1% SB3-14	50 mM Tris–HCl, pH 8.0	C14SB	ND	ND	ND	Overexpression of <i>H. influenzae</i> gene in <i>B. subtilis</i> (Went into IB)	1996, [114]

(continued on next page)

Table 1 (continued)

Protein	MW (kDa); Topology; Oligomeric state	Denaturant	Other components of unfolding buffer	Method of refolding	Optimal refolding buffer	Refolding detergent	Folding efficiency	Conformation of D-states in denaturant ^a	Aggregation state of D-states ^a	Source	Year published, Reference
<i>Rps. Blastica</i> porin	Not stated; predicted BB; predicted Trimer	8 M Urea	50 mM Tris-HCl, pH 8.0, 1 mM EDTA, 100 mM NaCl	Dilution	50 mM Tris-HCl, pH 8.0, 1 mM EDTA, 100 mM NaCl	10% LDAO micelles	ND	ND	ND	<i>E. coli</i> expression into IB	1996, [115]
Pea root plastid porin (a eukaryotic mitochondrial porin)	Not stated; predicted BB; Unknown	1% SDS	10 mM KPi, pH 7.0, 0.1 mM EDTA	Dilution	10 mM KPi, pH 7.0, 0.1 mM EDTA	2% (v/v) Genapol X-80	ND	Helical in 1% SDS (CD)	ND	<i>E. coli</i> expression into IB	1997, [116]
Pea root plastid porin (a eukaryotic mitochondrial porin)	Not stated; predicted BB; Unknown	8 M urea	10 mM KPi, pH 7.0, 0.1 mM EDTA	Dilution	10 mM KPi, pH 7.0, 0.1 mM EDTA	2% (v/v) Genapol X-80	ND	No regular structure (CD)	ND	<i>E. coli</i> expression into IB	1997, [116]
Chloroplast Toc75	Unknown	7 M urea plus 1.2% sodium <i>N</i> -lauroyl-sarcosinate	100 mM Tris-HCl, pH 8.0	Dilution to 3.2 M urea plus 0.6% (w/v) sodium <i>N</i> -lauroyl-sarcosinate, binding to a column, detergent exchange into Triton X-100	20 mM Tris, pH 8.0, 90 mM NaCl	sodium <i>N</i> -lauroyl-sarcosinate or Triton X-100	<10% (2/25 mg of IB)	ND	ND	<i>E. coli</i> expression of chloroplast Toc75	1998, [117]
<i>N. crassa</i> and <i>S. cerevisiae</i> VDAC	~35; predicted BB; Unknown	6 M GdnHCl	20 mM Tris-HCl, pH 8.0, 100 mM NaCl	Addition of 2% LDAO, dialysis	20 mM Tris-HCl, pH 8.0	2% LDAO	<10%	ND	ND	<i>E. coli</i> expression of <i>N. crassa</i> and <i>S. cerevisiae</i> genes	1998, [118]
<i>S. cerevisiae</i> Tom40	~40; predicted BB; Unknown	8 M urea	50 mM Tris-HCl, pH 8.0, 1 mM EDTA, 100 mM dithiothreitol	Tenfold dilution into Mega-9	10 mM MOPS/Tris pH 7.0, 1 mM EDTA, 100 mM DTT	Mega-9	ND	No regular structure	ND	<i>E. coli</i> expression of <i>S. cerevisiae</i> protein into IB	1998, [119]
OmpX	18; 8 stranded BB; Monomer	6 N GdnHCl	None	Dilution	Dilution	5% C8-POE	ND	ND	ND	<i>E. coli</i>	1999, [111]
OmpT	34; 10 stranded BB; Monomer	8 M urea	50 mM glycine, pH 8.3	Boil 5 min, cool on ice, quick dilution	1.6 M urea, 10 mM glycine pH 8.3	C14SB	90%	ND	ND	<i>E. coli</i>	2000, [120]

DAGK (C46A, C113A)	13; 3 Helices; Trimer	6.5 M urea + 1% formic acid	150 mM NaCl	200-fold dilution	75 mM PIPES, 50 mM LiCl, 0.1 mM EDTA, 0.1 mM EGTA, 1 mM DTT, 1 mM PEP, 0.5 mM NADH, 3 mM ATP, 15 mM MG(II), 3 mM DBG, pH 6.8	1 mol % DM, 3 mol % CL, 5 mol % dihexanoylglycerol as the phosphoryl acceptor	46%	Native-like CD	Monomer	<i>E. coli</i>	2001, [38]
DAGK (C46A, C113A)	13; 3 Helices; Trimer	8 M GdnHCl + 1% formic acid	150 mM NaCl	200-fold dilution	Same as row above	1 mol % DM, 3 mol % CL, 5 mol % dihexanoylglycerol as the phosphoryl acceptor	6%	No regular structure (CD)	Monomer	<i>E. coli</i>	2001, [38]
DsbB	19; 4 Helices; Monomer	SDS	25 mM NaPi, pH 8, 100 mM NaCl, 25 °C	Titration	25 mM NaPi, pH 8, 100 mM NaCl, 25 °C	DM	>90%	Significant helical structure (CD)	ND	<i>E. coli</i>	2003, [63]
OmpG	32; 14 stranded BB; Monomer	8 M urea	10 mM Tris, pH 8.0	Addition of detergent to water soluble unfolded ensemble	4% βOG, 1.5 M urea, 10 mM sodium borate, pH 9.0, 37 °C	4% βOG	>90%	No regular structure in 8 M urea, 10 mM NaP, pH 8.0 (CD)	ND	<i>E. coli</i>	2003, [37]
Tobacco light- harvesting chlorophyll a/b protein complex	Not stated; Helical; Unknown	1% SDS	None	Tenfold quick dilution with vortexing	50 mM borate pH 9.0, 12.5% sucrose, 10 mM βME	2.5% (w/v) βOG, 0.55 mM PG	>50%	27% helix (CD)	ND	Tobacco gene expressed in <i>E. coli</i>	2003, [72]
Tobacco light- harvesting chlorophyll a/b protein complex	Not stated; Helical; Unknown	6 M GdnHCl	None	Tenfold quick dilution with vortexing	Same as row above	2.5% (w/v) βOG, 0.55 mM PG	>50%	No regular structure (CD)	ND	Tobacco gene expressed in <i>E. coli</i>	2003, [72]
beta1 + beta2 TM barrel domain of AIDA	47.5; predicted BB; Unknown	8 M urea	50 mM Tris, pH 8.0, 100 mM NaCl	Mixing	50 mM Tris, pH 8.0, 100 mM NaCl	oPOE	50%	ND	Monomeric	<i>E. coli</i>	2005, [98]

^a Refers to denaturing condition in same row, before dilution of it.

Table 2
Membrane protein folding conditions observed using lipid bilayers

Protein	MW (kDa); Topology; Oligomeric state	Denaturant	Other components of unfolding buffer	Method of refolding	Optimal refolding Buffer	Refolding lipid	Folding efficiency	CD of D-states in denaturant ^a	Aggregation state of D-states ^a	Source	Year published, Reference
Bacteriorhodopsin	27; 7 Helices; Trimer	SDS	10 mM NaPi, pH 8.0, 0.025% sodium azide	Addition of retinal, soybean lipids and deoxycholic acid, dialysis	10 mM NaPi, pH 8.0, 0.025% sodium azide	Formed by detergent dialysis	>90%	~50% helical structure (CD)	Monomer	Purple membrane from <i>H.</i> <i>halobium</i>	1981, [15]
Bacteriorhodopsin	27; 7 Helices; Trimer	SDS	50 mM NaPi, pH 6.0	Dilution	50 mM NaPi, pH 6.0	Extruded 50 nm DMPC, DOPC, or DPoPC vesicles, all containing 0.1% SDS	>90%	~50% helical structure (CD)	Monomer	Purple membrane from <i>H.</i> <i>halobium</i>	1999, [55]
OmpA	35; 8 stranded BB; Monomer	8 M urea	20 mM KPi, pH 7.3	Dilution	10 mM KPi, pH 7.3	Small (sonicated) DMPC vesicles at 30 °C	40–50%	No regular structure (CD)	ND	<i>E. coli</i>	1992, [94]
OmpA	35; 8 stranded BB; Monomer	8 M urea	20 mM KPi, pH 7.3	Dilution	20 mM glycine, pH 10.0	Small (sonicated) DMPC vesicles at 30 °C	>95%	No regular structure (CD)	ND	<i>E. coli</i>	1995, [95]
OmpA	35; 8 stranded BB; Monomer	8 M urea	None	Dilution	10 mM glycine, pH 8.3, 1 mM EDTA, 150 mM NaCl	Sonicated DOPC vesicles at 30 °C or 40 °C	>95%	No regular structure (CD)	ND	<i>E. coli</i>	1996, [121]
OmpA	35; 8 stranded BB; Monomer	8 M urea	None	Dilution	10 mM borate, pH 10, 2 mM EDTA	100 nm LUVS composed of <i>di</i> C ₁₀ PC or <i>di</i> / C ₁₁ PC or <i>di</i> C ₁₂ PC. No folding was observed in LUVs of <i>di</i> C _{18,1} PC or <i>di</i> C ₁₄ PC	>95%	No regular structure (CD)	ND	<i>E. coli</i>	2002, [93]
OmpA equilibrium titration experiments	35; 8 stranded BB; Monomer	8 M urea	None	Dilution	10 mM glycine, pH 10.0, 2 mM EDTA	Many varied conditions using sonicated DOPC/ DOPG SUVs as a basis composition for additional lipids	>95%	No regular structure (CD)	ND	<i>E. coli</i>	2004, 2006, [24,122]
OmpF	35; 16 stranded BB; Trimer	8 M urea	20 mM KPi, pH 7.3	Dilution	20 mM NaPi, pH 6.5	Small (sonicated) DMPC vesicles at 10 or 30 °C	0% at 10 °C, <20% at 30 °C	No regular structure (CD)	Monomer	<i>E. coli</i>	1996, [109]
OmpF	35; 16 stranded BB; Trimer	8 M urea	20 mM KPi, pH 7.3	Dilution	20 mM NaPi, pH 6.5	DMPC; folds equally well into 30 or 180 nm vesicles	15% trimer	No regular structure (CD)	ND	<i>E. coli</i>	1996, [109]

DAGK (C46A,C113A)	13; 3 Helices; Trimer	6.5 M urea + 1% formic acid	150 mM NaCl	200-fold dilution	75 mM PIPES, 50 mM LiCl, 0.1 mM EDTA, 0.1 mM EGTA, 1 mM DTT, 1 mM PEP, 0.5 mM NADH, 3 mM ATP, 15 mM MG(II), 3 mM DBG, pH 6.8	POPC, 50 nm unilamellar vesicles (extruded)	26%	Native-like CD	Monomer	<i>E. coli</i>	2001, [38]
DAGK (C46A,C113A)	13; 3 Helices; Trimer	8 M GdnHCl + 1% formic acid	150 mM NaCl	200-fold dilution	Same as above row	POPC 50 nm unilamellar vesicles (extruded)	1%	No regular structure (CD)	Monomer	<i>E. coli</i>	2001, [38]
KCSA	19; 2 Helices; Tetramer	Boiling in SDS	Not stated	Dilution	100 mM Tris, pH 7.5, 200 mM NaCl, 15 mM KCl, 10% glycerol, 10 mM DTT	Soybean lipids	~30% Tetramer	ND	ND	<i>E. coli</i> expression of a synthetic gene for the <i>S. lividans</i> protein	2002, [123]
FomA	40; BB; Unknown	10 M urea	10 mM bo rate, pH 10, 2 mM EDTA	14× quick dilution	10 mM borate, pH 10, 2 mM EDTA	di_{10} PC or $di_{18:1}$ PC LUVs or SUVs (sonicated)	>90% in diC_{10} PC SUVs or LUVs, ~50% in $diC_{18:1}$ PC SUVs, <10% in $diC_{18:1}$ PC LUVs	No regular structure (CD)	ND		
<i>Fusobacterium nucleatum</i> ORF expressed in <i>E. coli</i>	2006, [39]										
hVDAC1	31; BB; Unknown	8 M urea	100 mM Tris, pH 8.0, 10 mM DTT, 1 mM EDTA	40-fold dilution	10 mM citrate, pH 3.0, 2 mM EDTA	diC_n PC 100 nm LUVs (extruded), $n = 10-14$	92-94% in diC_{12} PC LUVs	No regular structure (CD)	ND	Human ORF expressed in <i>E. coli</i>	2007, [89]
OMPLA	31; 12 stranded BB; Monomer/ Dimer	8 M urea	10 mM borate, pH 10.0, 2 mM EDTA	Dilution	10 mM borate, pH 10.0, 2 mM EDTA, 1 M urea	$c/;C_{10}$ PC100 nmLUVs (extruded)	>90%	No regular structure (CD)	ND	<i>E. coli</i> expression of mature protein into inclusion bodies	2007, NK Burgess, A.M. Stanley and K.G. Fleming, unpublished observations

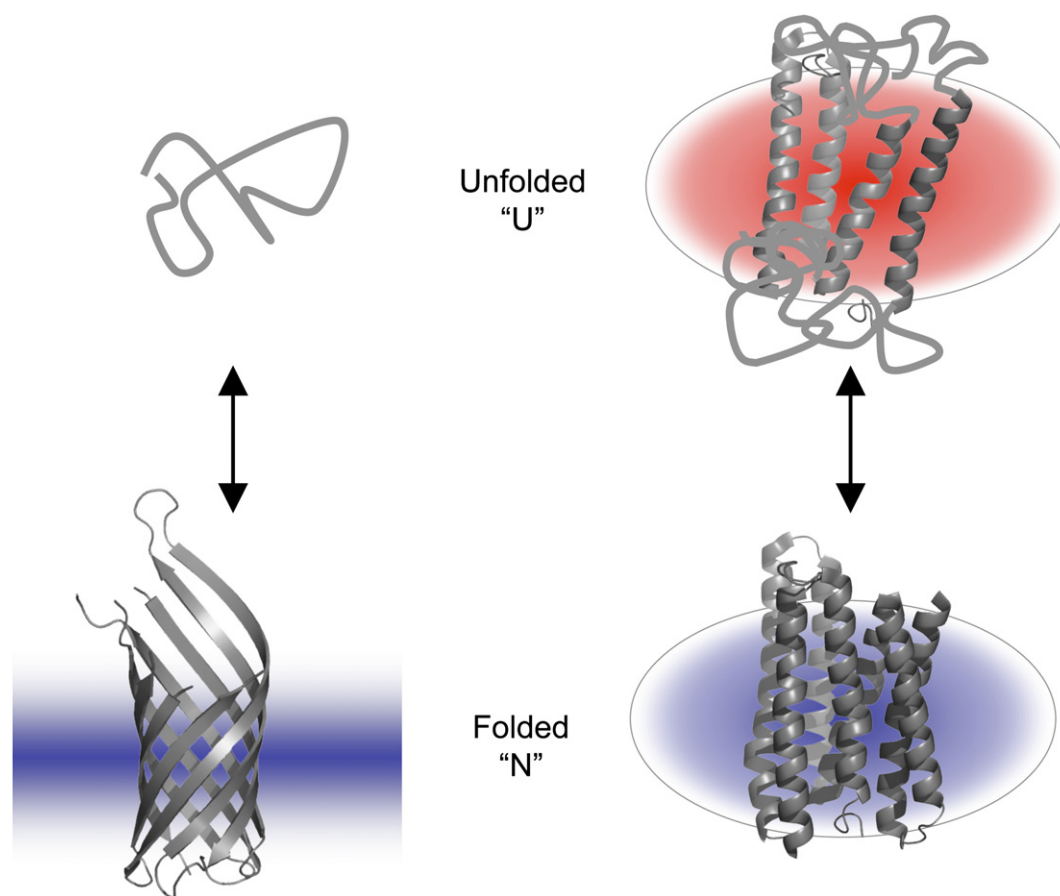


Fig. 2. A cartoon showing two equilibrium folding reactions that are studied *in vitro*. The left side shows the folding reaction typical of OmpA that occurs between a canonically unfolded protein in aqueous solution (starting from a urea-solubilized state) and the native state in a bilayer (indicated by the rectangle). The right side shows the folding reaction typical of polytopic helical proteins that occurs between two micellar states: a partially unfolded SDS-denatured state (red micelle) and the native state in different detergent or detergent/lipid mixed micelles (blue) that stabilize the native state.

state could be re-attained. Neither the scanning rate dependence nor the cooling profile were explored in this study, but it is notable that the reaction may be reversible. What is different about OmpG? It has a simpler topology and lower molecular weight than many of the proteins examined in previous thermal denaturation investigations. This work suggests that temperature warrants further exploration and that it might be a useful denaturant for thermodynamic studies for some membrane proteins.

Chemical denaturants

The addition of small molecule chemical denaturants is another approach employed for protein stability studies *in vitro*. The chemical denaturants most useful in soluble protein folding studies, guanidine hydrochloride (GdnHCl) and especially urea, have been widely used in refolding studies of membrane proteins. As noted in Tables 1 and 2, these chemicals have predominantly been successful in the refolding of transmembrane β -barrels [20] although the helical proteins light harvesting chlorophyll a/b protein (LHCIb) and diacylglycerol kinase (DAGK) have been refolded using urea as the denaturant.

However, even with β -barrels these denaturants are not universally effective, and their application to any particular membrane protein needs to be experimentally validated. One obstacle to their use appears to be their inability to solubilize any particular membrane protein in the absence of detergent micelles or lipids. This may be one problem with the helical proteins as the dissolution of DAGK in 8 M urea requires the addition of 1% formic acid for solubility of its denatured state ensemble [38]. Since urea and GdnHCl occur more frequently in protein folding studies of transmembrane β -barrels (Tables 1 and 2), this class of proteins might have a technical advantage in this respect in that their denatured states might generally have increased solubility in either urea or GdnHCl solutions lacking lipid vesicles or detergent micelles. Their increased solubility might be rationalized by the differences in the distribution of residues in the primary amino acid sequences for these two classes of membrane proteins: a predominantly α -helical transmembrane protein contains continuous stretches of hydrophobic amino acids whereas the sequence of a transmembrane β -barrel protein contains alternating hydrophobic and hydrophilic residues. In the unfolded state, a helical protein will still have local regions

of concentrated hydrophobic residues that compromise technical manipulations as well as solubility in aqueous solutions, whereas the unfolded β -barrel protein with interspersed hydrophilic residues can adopt soluble conformations in water [39] and in solutions containing chemical denaturants (for a review, see [20]). Still, the solubility of any particular transmembrane β -barrel in chemical denaturants is not guaranteed: For example, we have cloned and expressed the *E. coli*, *C. jejuni*, and *H. pylori* homologues of outer membrane phospholipase A (OMPLA). They have similar molecular weights and predicted numbers of transmembrane strands; pairwise comparisons show that the sequences of these proteins are $\sim 40\%$ similar and $\sim 20\%$ identical to each other yet only the *E. coli* homologue is soluble in both urea and GdnHCl. The *C. jejuni* protein is soluble in 6 M GdnHCl but not urea, and the *H. pylori* protein is only negligibly soluble in either urea or GdnHCl (A.M. Stanley and K.G. Fleming, unpublished observations). Thus, even with evolutionarily conserved protein sequences, the initial step of solubilizing the denatured state cannot be assumed but must be experimentally explored.

Even when these traditional denaturants solubilize a particular membrane protein, a second challenge with their usage is that they may not necessarily be denaturing to it. Noticed as early as the mid-1970s [40], Tanford subsequently postulated that “resistance to denaturation” might in fact be a characteristic of membrane-spanning regions of proteins [41]. Several archetypical membrane proteins retain significant fractions of secondary structure, even when exposed to high concentrations of GdnHCl [41,42]. Later, Chen and Gouaux concluded that neither 8 M urea nor 6 M GdnHCl perturbed the tertiary structure of bacteriorhodopsin: upon exposure of folded BR to either of these denaturants there were only small changes in the 555 nm retinal absorbance peak, a sensitive reporter of tertiary structure [43]. Moreover, in an inverse experiment, they showed that SDS-solubilized (partially unfolded) bacteriorhodopsin can refold into DMPC/CHAPSO mixed micelles *even in the presence of 7 M urea* [43]. Similarly, the KcsA potassium channel is not denatured by GdnHCl or urea but requires $>30\%$ trifluoroethanol to disrupt its helical secondary structure and destabilize the native tetramer [44,45]. As previously observed in the temperature denaturation studies, chemical denaturants can also partially destabilize membrane proteins by solely denaturing their aqueous regions as demonstrated by the transmembrane domain of the anion transporter protein, which retains 70% of its CD signal at 222 nm in presence of 4 M GdnHCl, even though its soluble domain displays a spectroscopic signal consistent with random coil [33].

This inability of urea or GdnHCl to promote the unfolded states of membrane proteins is not unique to the helical proteins, and it can depend on the lipid environment. Kleinschmidt observed that native OmpA in *diC*₁₂PC lipid vesicles is not denatured by 8 M urea even after a 12 day incubation at 40 °C [46]. In this latter case,

there must be a kinetic component at play because OmpA is highly soluble in 8 M urea in the absence of lipid vesicles, stays denatured at this urea concentration when vesicles are added, and can refold following dilution of urea in the presence of lipid vesicles [46]. The relative contributions of kinetic and thermodynamic components are not clear in the case of BR as there are no reports of BR solubility (or insolubility) in urea in the absence of detergent micelles or lipids, although a maltose binding protein-bacterioopsin fusion protein is soluble in 8 M urea or in water [43]. It might also be that the incubation times in the Gouaux study were 2 h at room temperature, which might not have been long enough for true equilibrium to be reached although the authors do note that the absorbance measurement stabilized within that time period.

In addition to urea and GdnHCl, another effective and widely used denaturant for membrane protein studies is sodium dodecyl sulfate (SDS). SDS is a well established denaturant of soluble proteins (e.g., SDS-PAGE), although it is not generally used in soluble protein stability studies. SDS can often, but not always [47], lead to the loss of native structures of helical membrane proteins. Above the critical micelle concentration and in detergent micelle or detergent/lipid mixtures SDS maintains solubility of membrane proteins in the absence of strong acid or base. Notably, SDS does not appear to be strongly destabilizing to folded transmembrane β -barrels at ambient temperatures; it is currently not known whether this is a consequence of kinetic or thermodynamic effects, however, the equilibrium thermodynamic use of SDS as a denaturant has been restricted to helical membrane proteins as it can denature this class of proteins at room temperature within an experimentally accessible time scale.

The use of SDS to promote the denatured state ensemble has been critically important for the many studies on bacteriorhodopsin, the polytopic helical membrane protein whose stability and folding has most extensively investigated. Huang found the SDS-denatured state to be an essential intermediate between the acid unfolded and the native states of bacteriorhodopsin [15]. Booth and coworkers have extensively used the SDS-denatured state as a starting point for many kinetic studies querying the influence of the lipid composition on the rate constant of acquisition of native structure [48–58]. Bowie and colleagues determined the free energy perturbations arising from single amino acid substitutions in helix B of bacteriorhodopsin in a mixed micelle system for which the SDS-denatured form provided the reference state [59]. SDS solubilization facilitated folding studies on additional helical membrane proteins including the light harvesting complex [60–62], the disulfide bond reducing protein DsbB [63], as well as a landmark study on DAGK in which Lau and Bowie observed that its stability depended linearly on the mole fraction content of SDS in an SDS/DM mixed micelle solution [25], providing the first evidence that the Santoro and Bolen linear extrapolation analysis [22] approach could be applicable to analysis of membrane protein stabilities.

Denaturants and the structures of the denatured state ensembles

The choice of denaturant has been shown to profoundly affect the conformations that characterize the denatured state ensemble (D-states); the effects can vary widely with the protein of study and the denaturant. Since the D-states serve as one reference point for interpretation of experimental protein folding results, it is important to consider the structural and energetic properties of this ensemble.

The denatured state ensemble induced by urea or GdnHCl

Almost everything known about denatured state ensembles in high concentrations of urea or GdnHCl is based on experimental work carried out on soluble proteins, and it may be a reasonable starting point for postulating properties of the D-states of transmembrane β -barrels dispersed in these solutions as there are two commonalities between transmembrane barrel and soluble proteins: (i) transmembrane β -barrels have a primary amino acid sequence that lacks—like soluble proteins—continuous hydrophobic stretches of amino acids; and (ii) transmembrane β -barrels tend to be highly soluble ($>10 \text{ mg ml}^{-1}$) in high concentrations of chemical denaturants in the absence of vesicles and detergent micelles, suggesting that urea may be a good solvent for them. On this basis, we can postulate that the denatured state ensembles of transmembrane β -barrel proteins are similar to those of soluble proteins and are composed of rapidly inter-converting conformations ([64] and references therein). Accordingly, their circular dichroism spectra suggest in all cases that these denaturants induce in a lack of regular structure resulting in the canonical unfolded, random coil state (Tables 1 and 2 and references therein) and as depicted for OmpA in Fig. 2. However, it is increasingly appreciated in soluble proteins that the members of the denatured state ensemble contain structures distinct from random coils despite their CD spectra [64,65]; D-states can be compact and can contain measurable amounts of residual structure [65–70]. While these latter questions are largely unexplored in transmembrane β -barrels, an NMR study of the denatured state ensemble of an outer membrane β -barrel protein (OmpX) demonstrated the presence non-random structure in 6.5 M urea [71], consistent with the general characteristics observed for soluble proteins.

The D-states of helical membrane proteins demonstrate a larger variation in their maintenance of native-like structure. Like transmembrane β -barrels, the denatured state ensembles of DAGK [38] and LHCIIB [72], induced by acidic and neutral GdnHCl, respectively, lack regular secondary structure as assessed by CD spectroscopy. In sharp contrast, the CD spectrum of the DAGK D-states induced by acidic urea appear native-like, even though the native trimeric protein is dissociated into monomers [38].

The denatured state ensemble induced by SDS

The denatured state ensemble of conformations induced by using SDS as a denaturant contains a much greater extent of residual structure. This might be expected as these D-states remain associated with a “lipidic” environment (e.g., SDS micelles) that is known to promote helix formation in proteins [73]. Thus, elements of secondary structure can persist: the CD spectra of folded and SDS-denatured bacterioopsin are similar [74], and the SDS-denatured state ensemble of bacteriorhodopsin is best characterized as a partially unfolded state that contains about half of the helix content found in the native state [75] as depicted in the unfolded cartoon of BR in Fig. 2. Even fragments corresponding to various transmembrane helices in BR can retain helical structure in SDS [76,77]. Similarly, the SDS-induced D-states of LHCIIB exhibit a strong negative circular dichroism (CD) peak at 220 nm, characteristic of helix content [72], and DAGK loses only 15% of the 222 nm band intensity when denatured by 10% SDS [25]. SDS as a denaturant therefore appears to be capturing only partially denatured states of helical membrane proteins—although it is worth recognizing that SDS might promote non-native α -helix structure, not necessarily native helix conformations.

An understanding of denatured state ensemble structures in SDS is further complicated by the question of whether or not CD is a reliable measure of secondary structure in SDS-solubilized samples. When studied using both NMR and CD under identical conditions, many peptides as well as transmembrane regions of membrane proteins demonstrate greater helix content in their NMR signals than in their CD signals [77–83]. The intensities of CD signals are well-known to be sensitive to factors such as helix length [84,85], and Renthall has suggested that the binding of SDS might alter the rotational strength of the peptide bond without inducing great changes in actual helix content [86]. As a consequence, there is the possibility that these denatured state ensembles may be even more native-like in their structures, and characterizing these D-states may deserve additional experimental scrutiny in model folding systems.

Even with this uncertainty in interpreting CD data, the structures of the denatured state ensemble define a reference point for interpreting the free energy change for folding reactions using this denaturant, and SDS as a denaturant is not as useful from the view of understanding the stability difference between an entirely unfolded polypeptide chain folding and the lipid-embedded native state. On the other hand, SDS may be thought of probing a different aspect of the folding reaction: SDS may promote a structural conformation consistent with the idea of a membrane-embedded intermediate and, if so, provides a mechanism to study the evolution of native structure from it. Assuming the secondary structure elements stabilized by SDS are native-like, SDS facilitates investigations of factors that influence the interactions between pre-formed

transmembrane helices in accordance with the “two-stage” thermodynamic model for membrane protein stability [87]. The sequence dependence of the protein interaction surface of glycophorin A transmembrane helix dimer and was in fact initially identified by a large scale mutagenesis study in which the dimer stability was evaluated in SDS using gel electrophoresis [47]. Investigations of helix–helix interactions within the framework of the two stage model in many detergent micelle environments and in lipid bilayers have been extensively discussed in a recent review [88].

The influences of the lipid bilayer on the denatured states induced by urea and GdnHCl

The chemically denatured states are not immune to the influences of the lipid bilayer. Even under strongly denaturing conditions, the inclusion of lipid vesicles or detergent micelles can alter the nature of the denatured state ensemble. Urea does not suppress the hydrophobic effect, and the denatured state ensemble of a membrane protein can either partially or fully partition onto the surfaces of vesicles in the absence of forming regular secondary structure. Tamm and coworkers showed that OmpA partitioning onto vesicles in 8 M urea is dependent on the lipid composition. The inclusion of 7.5 mol % of the anionic lipid palmitoyl-oleoyl-phosphatidylglycerol (POPG) in a background of palmitoyl-oleoyl-phosphatidylcholine (POPC) suppresses the surface partitioning of OmpA without inhibiting its folding. It is likely that the mechanism for this is electrostatic in nature since OmpA folds most efficiently under basic pH conditions and has an acidic isoelectric point; under folding titration conditions, it is negatively charged like the anionic POPG lipids, and the electrostatic interactions between the two molecules would be highly unfavorable. This “partitioning” step in folding has not been investigated in other proteins, but Tamm’s work may predict that vesicle partitioning of a polypeptide chain could be additionally influenced by the isoelectric point of the particular membrane protein under study as well as the buffer pH. It is therefore anticipated that both the protein sequence and the lipidic environment will influence this interaction, suggesting some level of specificity in this otherwise general partitioning step. Since GdnHCl is a charged denaturant, unlike urea, there could be differences in the ability of the denatured state ensembles to partition onto vesicles and therefore differences in the conformations present in the denatured state ensembles.

Populating the native state: finding conditions that facilitate efficient folding

Once solubilization conditions for the denatured state ensemble have been found, a second challenge in membrane protein stability studies *in vitro* is finding folding conditions that facilitate 100% efficient folding on a time scale compatible with experiments. This is a major hurdle

to be overcome because inefficient folding compromises the ability to correlate spectroscopic signals with the fraction folded in stability studies. Tables 1 and 2 show the conditions under which many membrane proteins fold and the efficiencies of folding are listed whenever they were available. However, aside from the many studies on OmpA and DAGK there are not many investigations that specifically explore this question of efficiency because obtaining sufficient quantities of folded protein for structural studies has been the goal of many refolding studies, especially those concerned with transmembrane β -barrels. Since expression into inclusion bodies can yields tens of milligrams of starting material, the yields of the folded population in these studies are usually sufficient for these experiments even though the efficiency is oftentimes less than 100%.

Methods used to assess folding in membrane proteins

The experimental approaches most frequently used to query the extent of native structure in membrane proteins are similar to those used in soluble protein folding studies. Circular dichroism spectroscopy plays a key role in assessing secondary structure content, although care must be taken to avoid artifacts from light scattering when vesicles are used. Fluorescence emission spectroscopy can also be extremely informative for ascertaining the polarity of the environment of tryptophan residues, however, there may be more ambiguity in the interpretation of membrane protein data. The partitioning of tryptophan side chains into the lipid bilayer—even in the absence of folding—places those residues in a less polar environment than water, and this can shift the maximum emission to shorter wavelengths much like that observed for the burial of tryptophan residues in the interiors of soluble proteins. The denaturant itself can also change the fluorescence emission properties of tryptophan [25], and a free tryptophan control is a prudent experiment to distinguish between these effects and changes in the protein conformation. In some cases, absorbance spectroscopy can be used as a probe for structure: DAGK shows a difference in its molar extinction coefficient when denatured by SDS [25]; and the retinal chromophore is a sensitive measure of BR structure. A fourth extensively employed experimental approach, SDS-PAGE, is a powerful method for evaluating the conformation of many transmembrane β -barrel proteins. Although there are a few exceptions [89], folded transmembrane β -barrels generally migrate faster on SDS-PAGE than do unfolded β -barrels as long as the samples are not boiled [90–92]. The increased migration is interpreted to reflect the compact shape of the barrel compared to the extended conformation characteristic of an unfolded protein. However, if boiled in SDS sample buffer, transmembrane β -barrels unfold and migrate at the positions expected for their molecular weights. This change in migration is referred to as “heat modifiability”, and is a convincing control for folding assays. Followed by densitometry of

the band intensities, SDS–PAGE analysis of transmembrane β -barrels is particularly informative as it reports the quantity fraction folded more directly than the spectroscopic methods. Over the course of an equilibrium titration or a kinetic experiment, SDS also appears to capture the conformational populations of transmembrane β -barrels present in solution and to “stop” the further progress of a folding or unfolding reaction. In the case of OmpA, Hong and Tamm have shown that its urea denaturation profiles as measured by SDS–PAGE and fluorescence emission spectroscopy (in the absence of SDS) overlay [24], suggesting that SDS does not strongly denature the folded state of OmpA at ambient temperatures. Finally, specific activity has also been used as a complementary approach in a few instances to evaluate the efficiency of folding. This is most useful in cases of membrane proteins with specific enzyme or binding activities, since the addition of substrates or cofactors, minimally perturbs the solution conditions under which folding is interrogated.

The effect of the hydrophobic environment on the kinetics and thermodynamics of folding efficiency

Folding efficiency is a function of both kinetics and thermodynamics: a folding reaction can appear negative or incomplete either because the kinetics are too slow for it to occur or finish on the experimental time scale or, alternatively, because the folding condition is one in which the folding free energy change is unfavorable or small; a combination of these effects can have the same outcome as depicted in the reaction coordinates shown in Fig. 3. Anything that influences the energies of either the folded or unfolded conformations or the transition between them can be manifested in the observable folding efficiency, and all of the mechanisms have been documented in experiments to date.

The hydrophobic environment employed in the experiment is a principal factor known to modify how efficiently a membrane protein folding reaction proceeds. This is unsurprising given that the properties of a membrane protein are intimately linked to those of its solvent. The lipid effects on folding efficiency are manifested in both transmembrane β -barrel and α -helical membrane proteins, and lipid appears to affect both the activation energy to folding as well as the final membrane protein stability. The variation in folding kinetics with different lipids or lipid superstructures can be large and can range from an observation of complete folding to one of no detectable folding over the same time period. For instance, in 2 h the transmembrane β -barrel OmpA folds efficiently into short chain diC_nPC ($n = 10, 11, \text{ or } 12$) LUVs but does not fold *at all* into long chain LUVs of $diC_{14}PC$ or $diC_{18:1}PC$ [93] whereas OmpA does fold into SUVs composed of $diC_{14}PC$ and $diC_{18:1}PC$ and other long chain lipids [94,95]. Since no folding is observed into LUVs this experiment cannot reveal whether the protein is unstable in these vesicles or whether the folding is just too slow to be

observed, however the latter interpretation is favored, since the folding rate constant is enhanced by SUVs. Hong and Tamm propose that the energy stored in the high curvature of small vesicles reduces the activation barrier to folding, which increases the rate constant of folding compared to LUVs of identical lipid compositions. In this scenario the broken green and solid gray activation barriers in Fig. 3A represent the folding conditions in LUVs and SUVs, respectively. Similarly, the folding rate constant of the SDS-denatured BR is affected by the lipid composition and is faster in lipids with a PC headgroup than those with a PE headgroup [96]. Collectively, these studies confirm that both hydrophobic thickness and elastic curvature forces can affect the folding rate constants and thus the efficiency of folding at a given time point.

Undoubtedly, the lipid composition must affect a membrane protein's equilibrium stability as well. In OmpA—the one case in which this has been studied—it is likely that the lipid composition tunes the free energy of the folded state as depicted by a modulation of the depth of the “folded” well in Fig. 3B. Using a host–guest lipid system within the architecture of SUVs in which the protein is unbound to lipids in the unfolded state, Hong and Tamm altered the bilayer thickness and lateral pressure by systematically constructing vesicles of defined compositions followed by determining OmpA stability [24]. By extrapolating the experimental observations to free energy values corresponding to 100% guest lipid, there is a clear stability trend with chain length: OmpA is least stable in bilayers composed of saturated short chain lipids and its stability increases linearly with bilayer thickness. In contrast, the stability of OmpA is greatest in mono-unsaturated C14 lipids, but decreases as the bilayer thickness is increased by using longer chain mono-unsaturated lipids. Paradoxically, the short chain saturated lipid compositions in which the folding kinetics were the fastest are those in which the stability is lowest, although the vesicle architectures were not the same in these two experiments. The effects of elastic curvature and lateral stress were further tested by a series of experiments in which lipids with a PE head group were used in the vesicle preparation. These lead to an enhancement of OmpA stability and were rationalized by the overall hourglass shape of the OmpA barrel [97]. Even though the increase in lateral pressure at the center of the bilayer reduces the efficiency of BR or DAGK folding, the increase may provide a better geometric match of the lipid forces to the architecture of the OmpA barrel. Since the shapes of β -barrels differ, this phenomenon may not be true for all transmembrane barrels, and future investigation on other molecular systems will test this idea.

Competing reactions that hinder productive folding

Additional circumstances that affect folding efficiency and that can thwart the investigators attempts to quantitatively study the folding process include competing

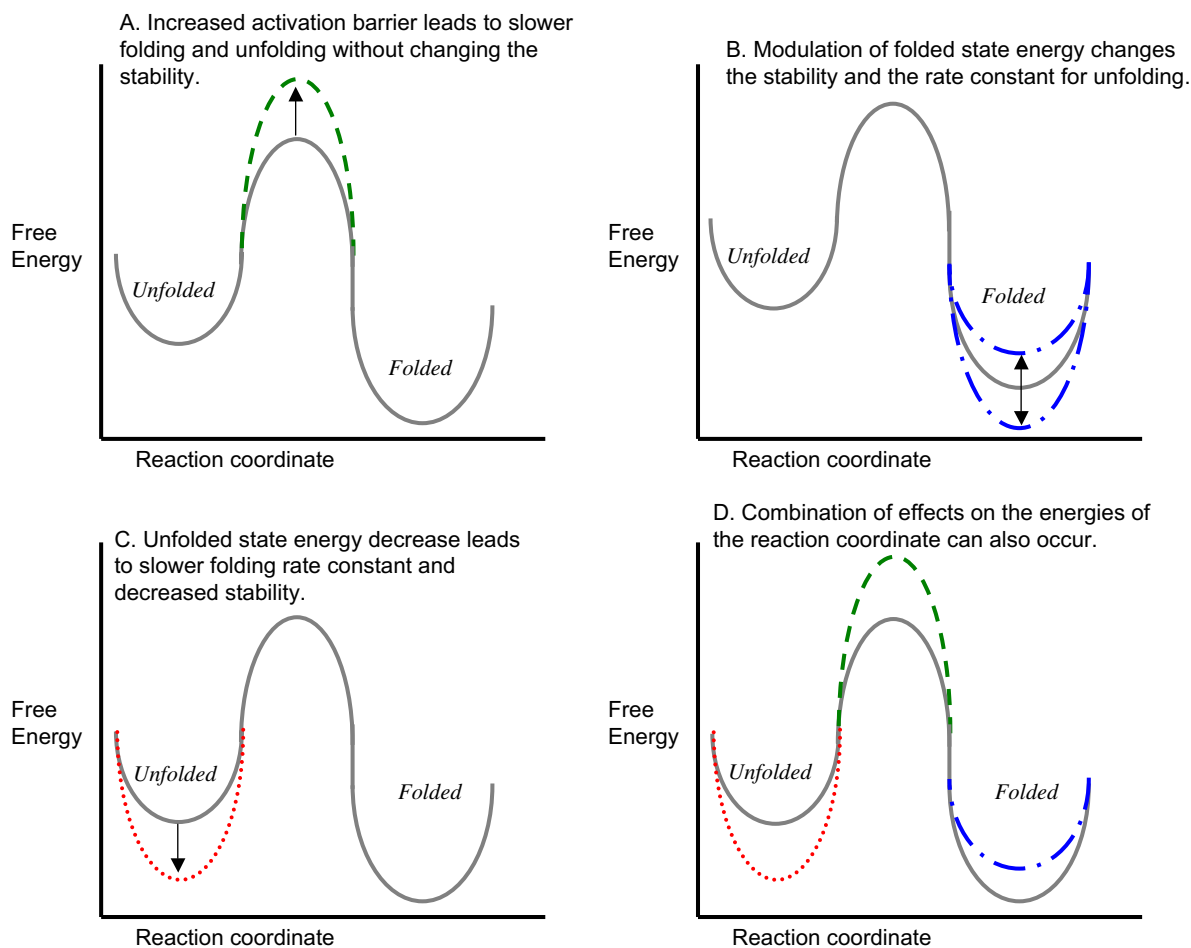


Fig. 3. Energy diagram of a hypothetical two-state folding reaction that depicts how the free energy of folding can be altered. The solid gray lines depict a “native” or reference situation in which the free energy of the folded state is lower than that of the unfolded state. Panel (A) shows an increase in the activation barrier (depicted by the broken green broken line) that occurs in the absence of perturbations to the energies of either the folded or unfolded states; this situation may be represented by the experiments on OmpA carried out in LUVs as compared to SUVs. Panel (B) shows modulation of the energy of the folded state. When the energy is increased as shown by the upper dot-dashed blue line, the free energy change for unfolding is reduced; this might represent the misfolding that is introduced by certain sequence variants of DAGK. When the energy is decreased as shown by the lower dot-dashed blue line, the free energy change for unfolding is increased and the protein is more stable, which represents the effect that long-chain lipids have on OmpA. Panel (C) shows a reduction in the energy of the unfolded state. The red dotted line shows how stabilizing the unfolded state reduces the free energy change for folding while also increasing the barrier to folding; this might be representative of how misfolding and/or aggregation slows the rate of membrane protein folding. Panel (D) shows a combination of the effects, which is also possible.

reactions, such as misfolding into kinetic traps, unproductive partitioning onto vesicle surfaces, or aggregation of the unfolded state upon dilution of the denaturant [98]. None of these on- and/or off-pathway intermediates are explicitly depicted in the simplified cartoon of Fig. 3C, but they collectively have the effect of lowering the energy of the unfolded states of a membrane protein as indicated by the dotted red line compared to the gray line. These processes thus increase the folding barrier, reduce the folding rate constant and decrease the overall folding efficiency at a given time point. These obstacles to folding efficiency can be enhanced or suppressed by the folding solution conditions as well as the starting conformations of the proteins in their denatured state ensembles. For instance, the folding efficiency of the helical protein LHCIIB is much greater from the SDS-denatured state than from the GdnHCl-denatured state [72]. There are differences between urea

and GdnHCl: the β -barrel OMPLA folds much more efficiently from a urea-denatured state than from a GdnHCl-denatured state [99]. The buffering pH is important: OmpA folding is most efficient at basic pH and drops to <70% at neutral pH [95].

In addition, studies on DAGK and sequence variants have shown that the tendency to misfold correlates inversely with apparent stability [100] and that this occurs independent of protein or lipid concentration. They conclude that amino acid changes can raise the free energy of the folded state without apparently affecting the free energy of the unfolded state and that this may also be the basis of protein misfolding. This interpretation is depicted by the upper blue (dot-dashed) line energy level of the folded state in Fig. 3 compared to the solid black line and predicts that sequence variants exhibiting this behavior would have faster unfolding rate constants.

While all of these misfolding phenomena may seem like annoying side reactions to be suppressed, there is a compelling biological relevance to motivate an understanding of the contexts and mechanisms causing membrane proteins to misfold as the incorrect folding of proteins is known to be associated with many human disease conditions [101]. Circumstances such as genetic mutations or stressed cellular conditions may readily lead to the misfolding of membrane proteins in the cell by any of these mechanisms even if the native form of the protein could potentially function if it were to be able to efficiently fold [101]. The activity of the $\Delta 508$ mutant cystic fibrosis channel is an example of a membrane protein that is functional, although the $\Delta 508$ mutation somehow prevents proper folding and trafficking under cellular conditions [102].

Is there a consensus “efficient” folding condition that can be used for membrane protein studies?

To facilitate comparisons of studies between different laboratories, members of the soluble protein-folding field have published a set of recommended conditions to be used whenever possible to standardize protein folding studies [103]. Membrane protein experiments carried out under a set of common conditions would similarly be useful in developing predictive models for membrane protein folding kinetics and stabilities. In addition, given the multitude of lipidic chemical compositions that can be envisioned, the parameter space for membrane protein folding studies is vastly larger than that of soluble proteins; winnowing the productive conditions down to a discrete and manageable number of possibilities would be advantageous to both theorists and experimentalists. However, it is clear from Tables 1 and 2 that identifying experimentally favorable folding conditions for any particular membrane protein can still be a laborious process of finding the right combination of lipid composition, lipid vesicle size, buffer, pH, and temperature. The folding studies to date provide some guidance in reducing the matrix: from the detergent studies in Table 1, it seems that there is a bias against anionic detergents for folding; from the few lipid studies in Table 2 it appears that small sonicated vesicles provide a kinetic advantage for folding studies of transmembrane β -barrel proteins. In addition, in all β -barrels but OmpF, short chain LUVs are a lipid environment in which protein folding has been observed in the laboratory, although we are not aware of any OmpF data demonstrating that short chain LUVs will *not* support folding *in vitro*. Nevertheless, it is currently not possible to predict *a priori* the conditions that will work for a given protein; for instance, there is no one common folding condition identified for the various microbial porins.

Establishing reversibility for extracting thermodynamic parameters

Only when denaturing and folding conditions have been identified can the investigator begin to extract ther-

modynamic parameters, the holy grail of stability studies. At this point, thermodynamic reversibility is a third challenge to the investigator that must be overcome and experimentally demonstrated in membrane protein folding studies. This is an essential prerequisite for extracting meaningful thermodynamic parameters to be used in deciphering the physical origins of membrane protein stability, and the importance of establishing reversibility cannot be overstated. As in soluble protein folding studies, it has been observed that membrane proteins respond cooperatively to the addition or removal of denaturant. Experimentally, this is manifested as a sigmoid-shaped curve in which the extremes represent the (usually linear) native and denatured state responses to the addition of denaturant and in which the steeply sloped region in between represents the cooperative transition from one conformation to the other. The important point to be recognized is that a sigmoid-shaped curve does not mean that a reaction is at equilibrium. Since the equations for analyzing these curves to obtain folding parameters are so well established [22,23], there is a temptation to forge ahead and fit the data using them, however, these equations have underlying assumptions about the reversibility of the process and it is worthwhile to think about them in further detail.

We will first consider where in the data the equilibrium constant can be known. Because the magnitudes of the observable signals can be so different when the data are obtained using different spectroscopic methods the experimental curve is often transformed into an expression of fraction folded. This curve also has a sigmoidal shape and transforms both the native and denatured baseline regions into ones with slopes of zero. This transformation from observed signal to fraction folded allows for CD and fluorescence data to be expressed on the same numerical scale and fitted with comparable weighting. As discussed previously, SDS-PAGE followed by densitometry of transmembrane β -barrel migration on gels yields data directly in terms of fraction folded on a scale of 0 to 1. Fig. 4 shows simulated data in this format; this could be either an unfolding profile if the starting point was on the left or a refolding profile if the starting condition was on the right. Note that the regions of ~ 0 slope at the extremes of this curve represent areas in the curve where only one species can be experimentally detected: at the left extreme, only $[N]$ is known as the fraction folded is >0.99 ; at the right extreme, only $[U]$ is known as the fraction unfolded is >0.99 . The free energy change for the protein folding reaction cannot therefore be experimentally determined in either of these regions because the ratio defining the equilibrium constant, $[U]/[N]$, cannot be calculated for these points. In contrast, the transition regions contain fractions of folded and unfolded protein that range from ~ 0.05 to ~ 0.95 , and both $[U]$ and $[N]$ can be known, depending on the precision of the experimental probe. It is therefore in this portion of the data where the equilibrium constant is experimentally observable. Demonstrating

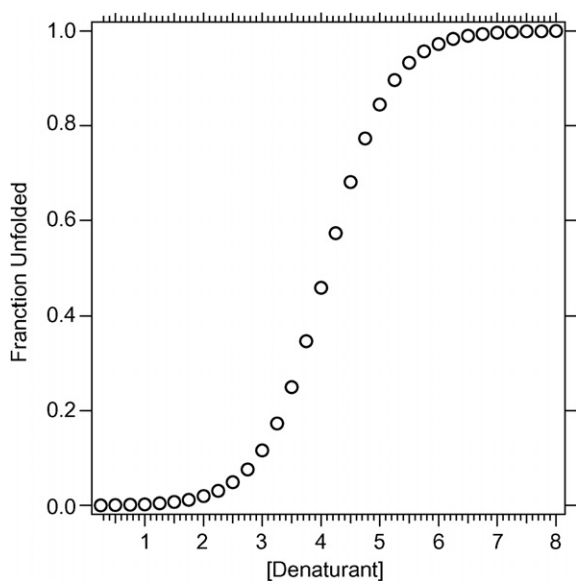


Fig. 4. A simulated sigmoidal response of a cooperative folding or unfolding response to denaturant. The data were simulated using a free energy of unfolding in water equal to $4.5 \text{ kcal mol}^{-1}$ and an m -value equal to $-1.1 \text{ kcal mol}^{-1} \text{ M}^{-1}$ and assuming a linear dependence of the free energy of unfolding on denaturant.

that the reaction has reached equilibrium within this transition region is the crucial control for these experiments.

How can one know that the reaction is at equilibrium? Thermodynamic parameters are state functions, which means that the equilibrium position is independent of the starting point. If the reaction between native and denatured conformations in this transition region is at equilibrium, the same transition should be obtained irrespective of the experimental origins. Stated another way, the denaturant dependence of a *folding* reaction, $U \rightarrow N$, must overlay upon the denaturant dependence of an *unfolding* reaction, $N \rightarrow U$. Only when these two curves coincide can reversibility be assured and meaningful thermodynamic parameters be extracted using the classical linear extrapolation analysis method. Even if each of the curves is sigmoid in shape, any hysteresis between them nullifies the ability to extract any thermodynamic parameters for stability [104].

There are two main experiments that can be used to establish reversibility: (i) the first is carry out two separate experiments and independently collect the folding and unfolding profiles; and (ii) the second is to carry out a denaturant-jump experiment starting from each of the endpoints and ending at the anticipated midpoint of the titration. There are three examples in the membrane protein literature that meet the reversibility criteria, and these are summarized in Table 3. Figs. 5 and 7 show this decisive data for two of the studies.

Fig. 5 shows the overlay of the folding and unfolding profiles for DAGK collected by Lau and Bowie [25]. In this experiment the SDS denatured state of DAGK could be folded upon the addition of DM (circles); conversely the folded form in DM micelles could be unfolded by the addi-

tion of SDS (squares). Having established reversibility, Lau and Bowie analyzed the titration data and showed that they are well described by the linear extrapolation equations widely used in the soluble protein-folding field [22], suggesting that—like soluble proteins—the free energy of unfolding is a linear function of the denaturant concentration.

An interesting feature of the DAGK denaturation by SDS is that two sigmoid transitions were observed using absorbance at 294 nm whereas only one was detected by circular dichroism; the CD transition overlaid upon the first absorbance transition, suggesting that it measured the same conformational process. Since absorbance changes upon denaturation arose mainly from tryptophan residues, Laue and Bowie used a series of DAGK sequence variants in which these were replaced, which allowed them to map the first and second absorbance transitions to residues W25 and W112, respectively. As shown in the topology cartoon of DAGK in Fig. 6, W25 is located in an amphipathic helix exposed to the aqueous solvent, and W112 is located inside the lipid bilayer. Since the two transitions were well separated, they could be fitted independently to give estimates for the free energies of unfolding in the absence of denaturant of the aqueous and membrane-embedded regions equal to 6 and 16 kcal mol^{-1} , respectively.

Fig. 7 shows the vital reversibility data for the transmembrane β -barrel OmpA: the same fraction folded is obtained at each point in a urea titration irrespective of whether the starting condition was native OmpA at low urea concentrations or fully unfolded OmpA in 8 M urea [24]. Hong and Tamm further demonstrated that the SDS–PAGE titration overlaid upon the titrations measured using CD and tryptophan fluorescence emission. The combination of these observations suggests that OmpA folding is two-state under these solution and lipid conditions. Indeed, OmpA is the only membrane protein whose folding free energy change between the fully unfolded state and the native state in lipid bilayers has been determined [24]. The use of the lipid composition, POPC/POPG (92.5/7.5 mol/mol) SUVs was key to this two-state behavior OmpA, since the negative electrostatic potential of POPG suppressed membrane-bound unfolded states. As a consequence, the binding and insertion into the vesicle, the secondary structure formation, and the compact barrel conformation all become one concerted equilibrium process. In the lipid composition above, the free energy of unfolding was $3.4 \text{ kcal mol}^{-1}$. This is far lower than that observed for the membrane-embedded region of DAGK, although the energetic contributions of the different environments employed in the two studies are unknown. As discussed previously, this equilibrium tool provided a means to quantitatively assess how the lipid bilayer modulates the stability of a membrane protein. Moreover, Hong et al. have recently probed the thermodynamic contributions of aromatic amino acids to the stability of OmpA using similar equilibrium titrations [105].

Table 3
Equilibrium titration studies of membrane protein stability

Protein	Denaturant	Other buffer components	Folding condition lipid or detergent	Data demonstrating reversibility	Conformation of D-states in denaturant	Free energy of unfolding in absence of denaturant	Year published and Reference
DAGK	SDS	10 mM PIPES, pH 7.0	1% DM	Overlay of folding and unfolding profiles	85% of native-like CD intensity at 222	16 kcal mol ⁻¹ for membrane-embedded region	1997, [25]
BR	SDS	10 mM NaPi, pH 6.0	15 mM DMPC, 16 mM CHAPSO	Overlay of folding and unfolding profiles	Significant α -helix structure, probably ~50% of native helicity (CD) [74]	ND	1999, [43]
OmpA	Urea	10 mM glycine, pH 10.0	Many lipid compositions: 92.5% POPC/7.5% POPG (mol/mol) SUVs were the basis for host:guest experiments in which other lipid types were introduced and their energetic effects determined	Overlay of folding and unfolding dependencies on denaturant (assayed by SDS-PAGE)	No regular structure (CD)	3.4 kcal mol ⁻¹ in basis lipid composition	2004, [24]

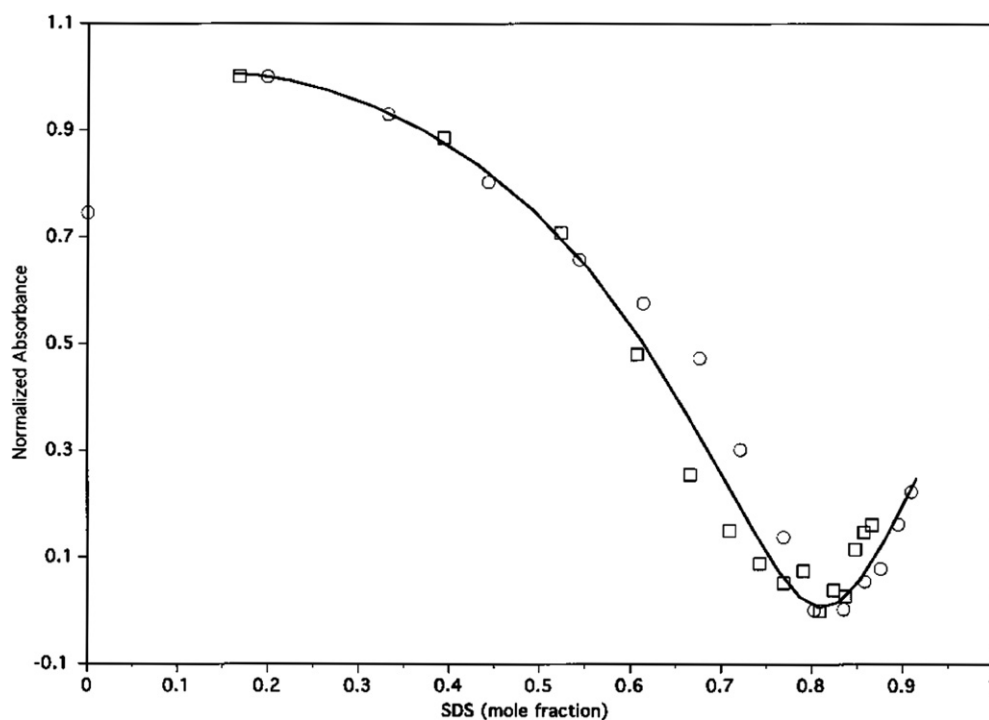


Fig. 5. Overlay of a folding and unfolding profile for DAGK. The circles show an unfolding profile in which SDS was titrated into a folded sample of DAGK in DM micelles; the squares show a refolding profile in which DM was titrated into unfolded DAGK in SDS micelles. Reprinted from Lau and Bowie [25]. Copyright American Chemical Society; used with permission.

In sharp contrast, Fig. 8 shows urea refolding and unfolding titrations of OmpA in *di*C₁₂PC LUVs [46]. Unlike the behavior of OmpA in POPC/POPG SUVs [24], the refolding and unfolding profiles in Fig. 8 exhibit marked hysteresis. While the refolding profile (solid points) shows a sigmoid-shaped cooperative folding response upon the removal of urea, the unfolding profile (open points) reveals a flat line in which the protein fails to unfold. The

circles represent data collected at time points of 1 and 12 days, respectively, and the samples were incubated at 40 °C. At the midpoint of the refolding curve where the fraction folded \cong 0.5, the fraction folded in the unfolding curve \cong 0. The reaction is therefore not at equilibrium. Even though each of the transitions has stabilized, they do not coincide: one or both of the reactions has a kinetic barrier to equilibrating between the two protein

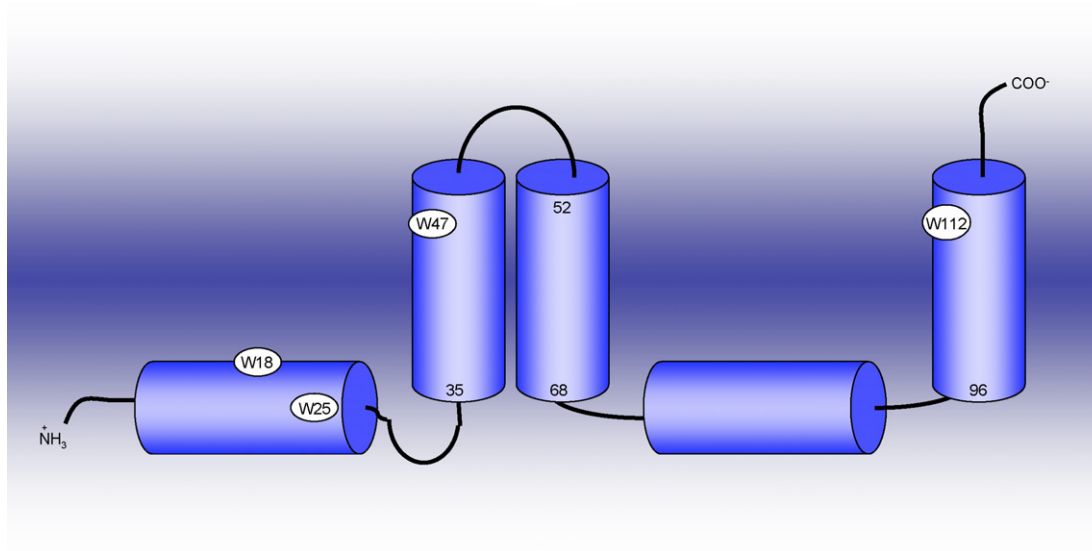


Fig. 6. Topological model of DAGK in a membrane. This figure is adapted from Lau and Bowie [25] and is based on the topology of DAGK derived by Smith et al. [124]. The identities and locations of the tryptophan residues used as spectroscopic probes for folding are indicated by the circles in the figure.

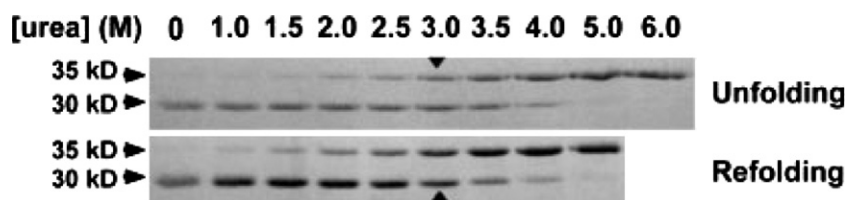


Fig. 7. Overlay of a folding and unfolding profile for OmpA. The fraction folded was assessed by migration of the transmembrane β -barrel on SDS-PAGE. The top panel shows unfolding of OmpA by the addition of urea; the bottom panel shows the refolding of OmpA by stepwise removal of urea. Reprinted from Hong and Tamm [24]. Used with permission.

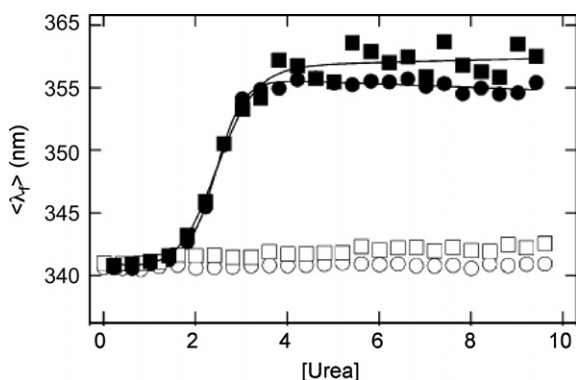


Fig. 8. An example of hysteresis in an OmpA folding titration carried out in *di*C₁₂PC LUVs. Refolding (solid symbols) and unfolding (open symbols) titrations of OmpA by urea. The data obtained after 1 or 12 days of incubation are shown in circles or squares, respectively. The abscissa shows the final urea concentration and the ordinate shows the spectral center of moment of the tryptophan fluorescence emission spectrum as described in the original article. The figure adapted from Pocanschi et al. [46]. Used with permission.

conformations. The stability of OmpA cannot be known from this experiment.

Implied in the above discussion is a description of experimental observations that do *not* meet the burden proving

thermodynamic reversibility. For instance, the recovery of an original native signal by jumping to folding conditions (the far left side of Fig. 4) subsequent to an unfolding titration experiment does not demonstrate reversibility in the transition region where the equilibrium constant is measured. The reverse is also true. Similarly when temperature is the denaturant, recovery of the original signal by cooling a sample following a thermal melt only shows that the protein is not irreversibly denatured; this observation alone provides no evidence that the transition region is an equilibrium one and that the T_m obtained in the thermal melt is thermodynamically relevant. In sum, in these relatively early days of folding proteins into lipids and trying to find conditions under which meaningful thermodynamic parameters can be extracted, it is critical that both unfolding and refolding profiles be collected and compared in order to validate the findings.

Another factor in demonstrating reversibility is determining the time required to reach equilibrium. It has been observed that the folding rate constants for membrane proteins into lipid bilayers can be manyfold longer than the folding rate constants for soluble proteins of similar molecular weights. It is also worth considering that the folding and unfolding rate constants are functions of the

denaturant concentrations. Under *folding* conditions, the folding rate constant is fast and dominates the time to equilibrium, and the unfolding rate constant is slow; the situation is reversed under *unfolding* conditions. At the midpoint of the titration, however, both the folding and unfolding rate constants are somewhat slow; accordingly, the time to equilibration is longest at the midpoint and can be manyfold slower than the time to equilibration at either of the endpoints; the V-shape of a chevron plot is a good representation of this phenomenon for two-state folders. Therefore, especially if they do not initially coincide, each folding and unfolding profile must be collected as a function of time with an emphasis on determining the time-to-equilibrium at the midpoint. For transmembrane β -barrels studied to date this can mean hours to days, however, the folding rate constants for SDS-denatured helical proteins may in fact be faster and on the order of seconds or less as indicated by kinetics studies of BR and DAGK [38].

Prospects

Stability studies on folding membrane proteins into lipid bilayers have historically focused on two membrane proteins: bacteriorhodopsin and OmpA. Their amenability to laboratory manipulations has profoundly aided in developing protocols for denaturation, renaturation, and equilibrium and kinetic studies of membrane proteins in general. In addition, the helical protein DAGK has emerged as another model system whose folding thermodynamics and kinetics are robust to investigation.

To ultimately derive general thermodynamic and kinetic principles for folding, a breadth of molecular systems will need to be explored, but currently the number of new membrane proteins as targets for folding studies is increasing only at the rate of about 1.5 per year (Fig. 9). At this pace there will still be far fewer than 50 proteins under study a decade from now. Moreover, membrane protein studies to date are dominated by proteins of bacterial origin. In Tables 1 and 2, there are only a handful of eukaryotic proteins and only one human protein entry. In evolutionarily conserved sequences, studies on the bacterial ancestors may provide a model for the folding of the corresponding proteins in higher organisms, but there will be differences, too, and there is no substitute for data directly collected on any given protein.

There is also a need for an increased number of in-depth thermodynamic and kinetic studies that quantitatively probe membrane protein stabilities and folding pathways. These types of protein folding studies provide unique access to sequence–structure–stability relationships that will be useful in developing theoretical models with predictive value. These experiments inform the molecular determinants for folding from the perspectives of both the polypeptide sequence as well as the lipid bilayer chemical composition and architecture. Even though they can be tricky to successfully execute, the few examples that have

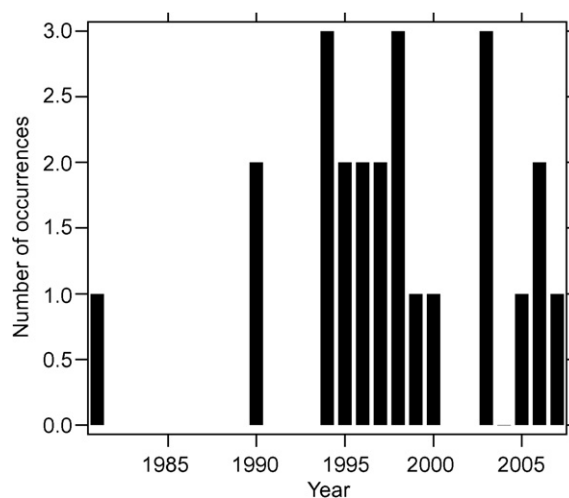


Fig. 9. The number of new proteins studied as a function of the publication year. Only the initial publication for any particular protein is counted. The total number of unique proteins in publications indexed by Pubmed through 2006 is 23, which corresponds to the initial entries for a protein in Tables 1 or 2. Note that denaturation-only studies of membrane proteins are included in neither this figure nor in Tables 1 and 2.

worked to date provide some guidance on how to approach this scientific quest.

It is also clear that detailed investigations of the *misfolding* of membrane proteins—such as the ones carried out on DAGK [38,100,106–108]—are rich in information on the challenges faced by the cell in producing natively folded membrane proteins. Not only will such studies provide biophysical insight into the forces acting on membrane protein polypeptides, they will inform on the roles that chaperones must play in preventing misfolding in a biological context. Understanding the competing events that hinder productive folding in simple model systems will be useful in ascertaining the behavior of more complex proteins in which such studies are not facile.

Acknowledgments

We gratefully acknowledge support from the National Science Foundation, (MCB 0423807 to K.G.F.), and we thank C. Preston Moon and Patrick Fleming for critical reading of the manuscript.

References

- [1] C.B. Anfinsen, *Science* 181 (96) (1973) 223–230.
- [2] S.S. Jaswal et al., *Nature* 415 (6869) (2002) 343–346.
- [3] S.H. White, W.C. Wimley, *Annu. Rev. Biophys. Biomol. Struct.* 28 (1999) 319–365.
- [4] M.C. Wiener, S.H. White, *Biophys. J.* 61 (2) (1992) 434–447.
- [5] J.E. Rothman, J. Lenard, *Science* 195 (4280) (1977) 743–753.
- [6] H. Kim et al., *Proc. Natl. Acad. Sci. USA* 103 (30) (2006) 11142–11147.
- [7] M. Rapp et al., *Science* 315 (5816) (2007) 1282–1284.
- [8] M. Rapp et al., *Nat. Struct. Mol. Biol.* 13 (2) (2006) 112–116.
- [9] W. Wickner, R. Schekman, *Science* 310 (5753) (2005) 1452–1456.
- [10] J.E. Mogensen, D.E. Otzen, *Mol. Microbiol.* 57 (2) (2005) 326–346.

- [11] J.G. Sklar et al., Proc. Natl. Acad. Sci. USA 104 (15) (2007) 6400–6405.
- [12] R. Voulhoux, J. Tommassen, Res. Microbiol. 155 (3) (2004) 129–135.
- [13] T. Wu et al., Cell 121 (2) (2005) 235–245.
- [14] J.L. Popot, D.M. Engelman, Biochemistry 29 (17) (1990) 4031–4037.
- [15] K.S. Huang et al., J. Biol. Chem. 256 (8) (1981) 3802–3809.
- [16] J.L. Popot, J. Trehwella, D.M. Engelman, Embo J. 5 (11) (1986) 3039–3044.
- [17] J.L. Popot, D.M. Engelman, Annu. Rev. Biochem. 69 (2000) 881–922.
- [18] R. Koebnik, Embo J. 15 (14) (1996) 3529–3537.
- [19] R. Koebnik, L. Kramer, J. Mol. Biol. 250 (5) (1995) 617–626.
- [20] S.K. Buchanan, Curr. Opin. Struct. Biol. 9 (4) (1999) 455–461.
- [21] C.N. Pace, Methods Enzymol. 131 (1986) 266–280.
- [22] M.M. Santoro, D.W. Bolen, Biochemistry 27 (21) (1988) 8063–8068.
- [23] M.M. Santoro, D.W. Bolen, Biochemistry 31 (20) (1992) 4901–4907.
- [24] H. Hong, L.K. Tamm, Proc. Natl. Acad. Sci. USA 101 (12) (2004) 4065–4070.
- [25] F.W. Lau, J.U. Bowie, Biochemistry 36 (19) (1997) 5884–5892.
- [26] C.G. Brouillette et al., Proteins 5 (1) (1989) 38–46.
- [27] C.G. Brouillette, D.D. Muccio, T.K. Finney, Biochemistry 26 (23) (1987) 7431–7438.
- [28] M.B. Jackson, J.M. Sturtevant, Biochemistry 17 (5) (1978) 911–915.
- [29] V.L. Shnyrov, P.L. Mateo, FEBS Lett. 324 (2) (1993) 237–240.
- [30] J.P. Allen et al., Proc. Natl. Acad. Sci. USA 84 (16) (1987) 5730–5734.
- [31] T. Haltia et al., Biochemistry 33 (32) (1994) 9731–9740.
- [32] S.R. Davio, P.S. Low, Biochemistry 21 (15) (1982) 3585–3593.
- [33] K. Oikawa, D.M. Lieberman, R.A. Reithmeier, Biochemistry 24 (12) (1985) 2843–2848.
- [34] L.K. Thompson et al., Biochemistry 28 (16) (1989) 6686–6695.
- [35] J.L. Eisele, J.P. Rosenbusch, J. Biol. Chem. 265 (18) (1990) 10217–10220.
- [36] T. Haltia, E. Freire, Biochim. Biophys. Acta 1241 (1995) 295–322.
- [37] S. Conlan, H. Bayley, Biochemistry 42 (31) (2003) 9453–9465.
- [38] J.K. Nagy, W.L. Lonzer, C.R. Sanders, Biochemistry 40 (30) (2001) 8971–8980.
- [39] C.L. Pocsanschi et al., J. Mol. Biol. 355 (3) (2006) 548–561.
- [40] T.L. Steck, J. Yu, J. Supramol. Struct. 1 (3) (1973) 220–232.
- [41] L.J. Rizzolo et al., Biochemistry 15 (16) (1976) 3433–3437.
- [42] D.M. Byers, J.A. Verpoorte, Biochim. Biophys. Acta 533 (2) (1978) 478–486.
- [43] G.Q. Chen, E. Gouaux, Biochemistry 38 (46) (1999) 15380–15387.
- [44] F.N. Barrera et al., Biochemistry 44 (43) (2005) 14344–14352.
- [45] E. van den Brink-van der Laan et al., Biochemistry 43 (14) (2004) 4240–4250.
- [46] C.L. Pocsanschi et al., Biophys. J. 91 (8) (2006) L75–L77.
- [47] M.A. Lemmon et al., J. Biol. Chem. 267 (11) (1992) 7683–7689.
- [48] S.J. Allen et al., J. Mol. Biol. 342 (4) (2004) 1279–1291.
- [49] S.J. Allen et al., J. Mol. Biol. 308 (2) (2001) 423–435.
- [50] P.J. Booth, Biochim. Biophys. Acta 1460 (1) (2000) 4–14.
- [51] P.J. Booth, A. Farooq, Eur. J. Biochem. 246 (3) (1997) 674–680.
- [52] P.J. Booth, A. Farooq, S.L. Flitsch, Biochemistry 35 (18) (1996) 5902–5909.
- [53] P.J. Booth et al., Nat. Struct. Biol. 2 (2) (1995) 139–143.
- [54] E.L. Compton et al., J. Mol. Biol. 357 (1) (2006) 325–338.
- [55] A.R. Curran, R.H. Templer, P.J. Booth, Biochemistry 38 (29) (1999) 9328–9336.
- [56] J.M. Kim et al., J. Mol. Biol. 308 (2) (2001) 409–422.
- [57] H. Lu, P.J. Booth, J. Mol. Biol. 299 (1) (2000) 233–243.
- [58] H. Lu, T. Marti, P.J. Booth, J. Mol. Biol. 308 (2) (2001) 437–446.
- [59] S. Faham et al., J. Mol. Biol. 335 (1) (2004) 297–305.
- [60] P.J. Booth, H. Paulsen, Biochemistry 35 (16) (1996) 5103–5108.
- [61] D. Reinsberg et al., Biochemistry 39 (46) (2000) 14305–14313.
- [62] D. Reinsberg et al., J. Mol. Biol. 308 (1) (2001) 59–67.
- [63] D.E. Otzen, J. Mol. Biol. 330 (4) (2003) 641–649.
- [64] E.R. McCarney et al., Crit. Rev. Biochem. Mol. Biol. 40 (4) (2005) 181–189.
- [65] N.C. Fitzkee, G.D. Rose, Proc. Natl. Acad. Sci. USA 101 (34) (2004) 12497–12502.
- [66] W.Y. Choy et al., J. Mol. Biol. 316 (1) (2002) 101–112.
- [67] O. Zhang, J.D. Forman-Kay, Biochemistry 34 (20) (1995) 6784–6794.
- [68] N.A. Farrow et al., Biochemistry 34 (3) (1995) 868–878.
- [69] O. Zhang, J.D. Forman-Kay, Biochemistry 36 (13) (1997) 3959–3970.
- [70] Y.K. Mok et al., J. Mol. Biol. 289 (3) (1999) 619–638.
- [71] H. Tafer et al., Biochemistry 43 (4) (2004) 860–869.
- [72] C. Yang, R. Horn, H. Paulsen, Biochemistry 42 (15) (2003) 4527–4533.
- [73] J.A. Reynolds, C. Tanford, J. Biol. Chem. 245 (19) (1970) 5161–5165.
- [74] R. Renthal, P. Haas, J. Protein Chem. 15 (3) (1996) 281–289.
- [75] E. London, H.G. Khorana, J. Biol. Chem. 257 (12) (1982) 7003–7011.
- [76] J.F. Hunt et al., Biochemistry 36 (49) (1997) 15156–15176.
- [77] K.V. Pervushin, A.S. Arseniev, FEBS Lett. 308 (2) (1992) 190–196.
- [78] J. Luneberg et al., J. Biol. Chem. 273 (44) (1998) 28822–28830.
- [79] C.A. MacRaild et al., Biochemistry 40 (18) (2001) 5414–5421.
- [80] R. Montserret et al., Biochemistry 39 (29) (2000) 8362–8373.
- [81] A. Rozek, G.W. Buchko, R.J. Cushley, Biochemistry 34 (22) (1995) 7401–7408.
- [82] R. Storjohann et al., Biochim. Biophys. Acta 1486 (2–3) (2000) 253–264.
- [83] G. Wang, W.D. Treleaven, R.J. Cushley, Biochim. Biophys. Acta 1301 (3) (1996) 174–184.
- [84] M. Goodman et al., Proc. Natl. Acad. Sci. USA 64 (2) (1969) 444–450.
- [85] W.C. Johnson Jr., Annu. Rev. Biophys. Biophys. Chem. 17 (1988) 145–166.
- [86] R. Renthal, Biochemistry 45 (49) (2006) 14559–14566.
- [87] J.-L. Popot, D.M. Engelman, Biochemistry 29 (17) (1990) 4032–4037.
- [88] K.R. Mackenzie, Chem. Rev. 106 (5) (2006) 1931–1977.
- [89] B. Shanmugavadivu et al., J. Mol. Biol. 368 (1) (2007) 66–78.
- [90] M. Behlau et al., J. Mol. Biol. 305 (1) (2001) 71–77.
- [91] K.P. Locher, J.P. Rosenbusch, Eur. J. Biochem. 247 (3) (1997) 770–775.
- [92] M. Schweizer et al., Eur. J. Biochem. 82 (1) (1978) 211–217.
- [93] J.H. Kleinschmidt, L.K. Tamm, J. Mol. Biol. 324 (2) (2002) 319–330.
- [94] T. Surrey, F. Jahnig, Proc. Natl. Acad. Sci. USA 89 (16) (1992) 7457–7461.
- [95] T. Surrey, F. Jahnig, J. Biol. Chem. 270 (47) (1995) 28199–28203.
- [96] S.J. Allen et al., J. Mol. Biol. 342 (4) (2004) 1293–1304.
- [97] A. Pautsch, G.E. Schulz, J. Mol. Biol. 298 (2) (2000) 273–282.
- [98] J.E. Mogensen et al., Biochemistry 44 (11) (2005) 4533–4545.
- [99] N. Dekker et al., Eur. J. Biochem. 232 (1) (1995) 214–219.
- [100] D. Mi et al., Biochemistry 45 (33) (2006) 10072–10084.
- [101] C.R. Sanders, J.K. Myers, Annu. Rev. Biophys. Biomol. Struct. 33 (2004) 25–51.
- [102] G.M. Denning et al., Nature 358 (6389) (1992) 761–764.
- [103] K.L. Maxwell et al., Protein Sci. 14 (3) (2005) 602–616.
- [104] D. Barrick, F.M. Hughson, Nat. Struct. Biol. 9 (2) (2002) 78–80.
- [105] H. Hong et al., J. Am. Chem. Soc. (2007).
- [106] J.K. Nagy, C.R. Sanders, Biochemistry 43 (1) (2004) 19–25.
- [107] K. Oxenoid, F.D. Sonnichsen, C.R. Sanders, Biochemistry 40 (17) (2001) 5111–5118.
- [108] B.M. Gorzelle et al., Biochemistry 38 (49) (1999) 16373–16382.
- [109] T. Surrey, A. Schmid, F. Jahnig, Biochemistry 35 (7) (1996) 2283–2288.
- [110] K. Dornmair, H. Kiefer, F. Jahnig, J. Biol. Chem. 265 (31) (1990) 18907–18911.
- [111] A. Pautsch et al., Proteins 34 (2) (1999) 167–172.

- [112] P. Van Gelder, H. De Cock, J. Tommassen, *Eur. J. Biochem.* 226 (3) (1994) 783–787.
- [113] H.L. Qi, J.Y. Tai, M.S. Blake, *Infect Immunol.* 62 (6) (1994) 2432–2439.
- [114] D. Dahan et al., *FEBS Lett.* 392 (3) (1996) 304–308.
- [115] B. Schmid, M. Kromer, G.E. Schulz, *FEBS Lett.* 381 (1–2) (1996) 111–114.
- [116] B. Popp et al., *Biochemistry* 36 (10) (1997) 2844–2852.
- [117] H. Rogl et al., *FEBS Lett.* 432 (1–2) (1998) 21–26.
- [118] D.A. Koppel et al., *J. Biol. Chem.* 273 (22) (1998) 13794–13800.
- [119] K. Hill et al., *Nature* 395 (6701) (1998) 516–521.
- [120] R.A. Kramer et al., *Eur. J. Biochem.* 267 (3) (2000) 885–893.
- [121] J.H. Kleinschmidt, L.K. Tamm, *Biochemistry* 35 (40) (1996) 12993–13000.
- [122] H. Hong, G. Szabo, L.K. Tamm, *Nat. Chem. Biol.* 2 (11) (2006) 627–635.
- [123] F.I. Valiyaveetil, R. MacKinnon, T.W. Muir, *J. Am. Chem. Soc.* 124 (31) (2002) 9113–9120.
- [124] R.L. Smith et al., *J. Bacteriol.* 176 (17) (1994) 5459–5465.